Biosensors and Bioelectronics 56 (2014) 204–209

Contents lists available at ScienceDirect

Biosensors and Bioelectronics

journal homepage: www.elsevier.com/locate/bios

Highly sensitive glucose biosensor based on Au–Ni coaxial nanorod array having high aspect ratio

Che-Wei Hsu [a], Gou-Jen Wang [a,b,*]

[a] Department of Mechanical Engineering, National Chung-Hsing University, Taichung 40227, Taiwan
[b] Graduate Institute of Biomedical Engineering, National Chung-Hsing University, Taichung 40227, Taiwan

ARTICLE INFO

Article history:
Received 24 October 2013
Received in revised form
1 January 2014
Accepted 17 January 2014
Available online 24 January 2014

Keywords:
Glucose biosensor
High-aspect-ratio Au–Ni coaxial nanorod array
Immersion gold
High sensitivity

ABSTRACT

An effective glucose biosensor requires a sufficient amount of GOx immobilizing on the electrode surface. An electrode of a 3D nanorod array, having a larger surface-to-volume ratio than a 2D nanostructure, can accommodate more GOx molecules to immobilize onto the surface of the nanorods. In this study, a highly sensitive Au–Ni coaxial nanorod array electrode fabricated through the integration of nano electroforming and immersion gold (IG) method for glucose detection was developed. The average diameter of the as-synthesized Ni nanorods and that of the Au–Ni nanorods were estimated to be 150 and 250 nm, respectively; both had a height of 30 μm. The aspect ratio was 120. Compared to that of a flat Au electrode, the effective sensing area was enhanced by 79.8 folds. Actual glucose detections demonstrated that the proposed Au–Ni coaxial nanorod array electrode could operate in a linear range of 27.5 μM–27.5 mM with a detection limit of 5.5 μM and a very high sensitivity of 769.6 $\mu A\ mM^{-1}\ cm^{-2}$. Good selectivity of the proposed sensing device was verified by sequential injections of uric acid (UA) and ascorbic acid (AA). Long-term stability was examined through successive detections over a period of 30 days.

1. Introduction

Diabetes is a global public health problem. Across the world, 347 million people suffer from this medical condition (Danaei et al., 2011). In general, the normal blood sugar concentration of a human ranges from 4.4 to 6.6 mM (Wang, 2008). A diabetes patient must monitor his/her blood glucose frequently, to avoid high blood sugar that leads to renal, retinal, and neural blood vessel complications (Turner et al., 1999). In 1962, the first enzyme electrode was released (Clark and Lyons, 1962), which was recognized as the pioneer of glucose detection. Since then, screen-printing techniques have been employed for the detection of glucose because of their low cost and easy-to-be-mass-produced process (Hill et al., 1996; Nagata et al., 1995). However, the relatively low sensitivity of 1.17 $\mu A\ mM^{-1}$ has limited the widespread applications of these techniques (Crouch et al., 2005).

Several characteristics are significant for an *in vitro* diagnostic (IVD) device, such as specificity, high sensitivity, low cost, ease for use, and small size. Furthermore, the samples should be disposable and should provide fast and stable results. In recent years, nanostructured electrodes have been widely used in diabetes detection devices because of their significant characteristics, such as high surface area, high surface activity, high catalytic efficiency, and strong adsorption. Gold nanomaterials are the most widely used electrode substrates of biosensors because of the high biocompatibility of gold. Huang et al. (2012) mixed glucose oxidase (GOx) and anilineboronic acid (ABA) with phosphate buffer saline (PBS), followed by depositing the mixed solution onto a gold nanoparticle (GNP)-distributed gold electrode. Chitosan was then added to further enhance the mechanical strength. A bioelectrode based on the nanofibers of electrospun gold with immobilized fructose dehydrogenase was developed by Marx et al. (2011). Electroless plating was employed to deposit GNPs onto the electrospun poly(acrylonitrile)-$HAuCl_4$ fiber so that a large surface-to-mass ratio of $0.32 \pm 0.04\ m^{-2}\ g^{-1}$ could be obtained. Cyclic voltammetry (CV) and biochemical assay were used for fixing GOx onto the electrode for glucose detection. Qiu et al. (2012) fabricated a nanostructured glucose biosensor based on an Au thin film electrode by using electrodeposition and galvanic replacement technology. This nanostructured electrode of the Au thin film enabled firm immobilization of GOx onto its surface. Lee et al. (2012) proposed a glucose biosensor based on a direct electron transfer approach. GNPs were used as the electrode for glucose detection by a direct transfer of electrons to GOx. Zheng et al. (2011) produced a GOx–GNP/egg shell membrane (ESM) electrode for glucose detection. It was reported that the response time of a GNP-containing electrode was half that of an electrode without GNP. Zhang et al. (2005) modified a plane Au electrode with a layer of GNP, followed by the covalent immobilization of GOx onto its surface to enhance the electron transfer between the GNPs and GOx. Liu et al. (2013a) presented an enzymatic glucose biosensor based on a three-dimensional gold nanodendrite (GND)-modified commercially available screen-printed electrode.

* Corresponding author at: National Chung-Hsing University, Graduate Institute of Biomedical Engineering, 250 Kuo-Kuang Road, Taichung 40227, Taiwan. Tel.: +886 4 22840725x320; fax: +886 4 22877170.
E-mail address: gjwang@dragon.nchu.edu.tw (G.-J. Wang).

0956-5663/$ - see front matter © 2014 Elsevier B.V. All rights reserved.
http://dx.doi.org/10.1016/j.bios.2014.01.023

In addition to the GNP, nanostructured carbon electrodes such as graphene, ordered mesoporous carbon (OMC), and carbon nanotube (CNT) have also been implemented for glucose detection. Lu et al. (2011) developed a non-enzymatic glucose biosensor based on Nafion, grapheme, and palladium nanoparticle (PdNP)-modified glassy carbon electrode (GEC). Effective detection could be achieved through the highly conductive grapheme and the high-potential catalytic PdNP. Kang et al. (2009) developed a graphene and chitosan nanocomposite-modified GEC for glucose detection. Xiao et al. (2009) used multi-walled carbon nanotubes (MWNTs) to develop a non-enzymatic glucose biosensor. An indium tin oxide (ITO) electrode coated with Nafion–silica, polyaniline-grafted multiwalled carbon nanotubes (MWNT-g-PANI), and GOx was developed for glucose detection (Gopalan et al., 2009).

Other nanostructured metal oxides such as ZnO, NiO, CuO, and TiO_2 have also been uses as the electrodes of glucose biosensors. Luo et al. (2013) integrated a Mn-doped ZnO multilayer structure and surface acoustic wave (SAW) for glucose detection. The advantages of this device included high sensitivity, high accuracy, and fast response time. Mu et al. (2011) pointed out that NiO is a suitable electrode material for a non-enzymatic glucose biosensor. Liu et al. (2013b) successfully mixed nanocrystals and nanocubics of Cu_2O with graphene nanosheets to develop a glucose biosensor. Zhang et al. (2011) utilized TiO_2 nanotubes (ϕ=120 nm) with GNPs deposited on the surface as an electrode for glucose detection.

An effective glucose biosensor requires a sufficient amount of GOx immobilizing on the electrode surface. An electrode of a 3D nanorod array, which has a larger surface-to-volume ratio than a 2D nanostructure, enables more GOx molecules to immobilize onto the surface of the nanorods. Hence, the sensing performance is expected to be highly enhanced. In this research, a novel glucose biosensor based on a Au–Ni coaxial nanorod array is proposed. The orderly uneven barrier-layer surface of an anodic aluminum oxide (AAO) membrane was used as the template for the fabrication of the Au–Ni coaxial nanorod array. A thin Au film was deposited on a side surface as the electrode for the further electroforming of the Ni nanorods. Nickel nanorods were electroformed into the nanochannels of the AAO template. Sodium hydroxide solution was then used for etching off the alumina of the AAO template to form a Ni nanorod array. The IG method was used for forming an Au shell, wrapping each individual Ni nanorod. The Au–Ni coaxial nanorod array was further used as a highly sensitive biosensor for the detection of glucose.

2. Material and method

The proposed Au–Ni coaxial nanorod array based glucose biosensor is schematically illustrated in Fig. 1. The Au–Ni coaxial nanorod array was adopted as the sensing electrode. Potassium ferricyanide and glucose oxidase were used as the mediator and enzyme, respectively. A Nafion thin film was used to prevent the action of some interfering substances.

2.1. Electrode fabrication and characterization

2.1.1. Electrode fabrication details

The sequential fabrication processes of the proposed high-aspect-ratio Au–Ni coaxial nanorod arrays as schematically represented in Fig. 2 are as follows: working electrode coating, nickel electro deposition, alumina etching, and gold plating by an IG method and glucose biosensor preparation. The details are described below.

(A) Working electrode coating
AAO membranes with a pore size of 0.1 μm and a thickness of 60 μm were purchased from Whatman, USA. A 100-nm-thick Au electrode for electroforming was coated onto one side of the AAO template using sputtering deposition. Next, a thin layer of nickel was added to the Au electrode surface by electroplating to increase the strength of the electrode.

(B) Nickel electroforming
Electroforming of nickel was carried out using a micro-electro forming system (EGG Instruments corporation/Model 263A) with a bulk nickel anode and the chromium and gold-coated AAO template as the cathode, under a constant current of 0.01 A at ambient temperature.

(C) Alumina etching
The sample was immersed in a 1-M sodium hydroxide solution at room temperature to etch out the alumina. High-aspect-ratio nickel nanorods were obtained.

(D) Immersion gold and annealing
Electroless nickel immersion gold (ENIG) is often used for printed circuit boards. It consists of an electroless nickel deposition covered with a thin membrane of immersion gold, which protects the nickel from oxidation. The samples were immersed in an IG solution at 85 °C for 3 min. Its chemical reaction was as follows:

$$Ni + 2Au(CN)_2 \rightarrow Ni^{2+} + 2Au + 4CN$$

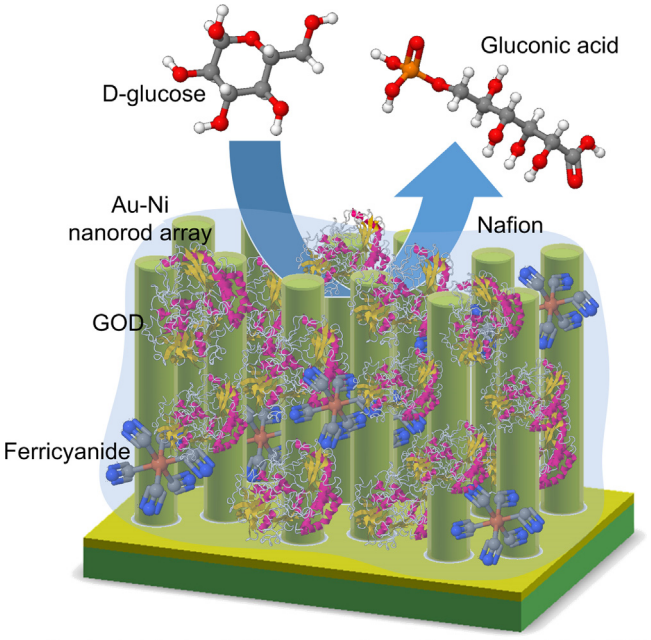

Fig. 1. Schematic representation of the proposed Au–Ni coaxial nanorod array based glucose biosensor.

The crystalline structure and mechanical properties of the Au shell of the nanorod were weak but could be improved by an additional annealing process. This procedure included the following: heating the sample to 120 °C at a rate of 6 °C min^{-1}, keeping the sample at this temperature for 2 h, and then cooling the sample in air to room temperature (Whitney et al., 1993).

2.1.2. Electrode characterization

The morphologies of the fabricated Au–Ni coaxial nanorod array electrode were observed using field emission gun scanning electron microscopy (FE-SEM) (JSM-6700F, JEOL, Japan). To ensure the consistency of measurement, the Au–Ni coaxial nanorod array electrode was bonded to a glass slide using a parafilm that

had a ϕ=6 mm hole in the center for solution contact. Cyclic voltammetry (CV) in a 0.1-M phosphate buffer (PB) with pH 7.0 using a SP-150 potentiostat (Bio-Logic, USA) was employed for the detection of the effective sensing areas.

2.2. Glucose biosensor preparation and glucose concentration detection

Potassium ferricyanide and glucose oxidase were sequentially coated onto the fabricated Au–Ni coaxial nanorod array, followed by the coating of a Nafion thin film for the isolation of the possible interferences. The glucose solution was then dropped onto the biosensor electrode. The detailed procedures for the glucose biosensor preparation are as follows:

(1) A potassium ferricyanide solution (10 μL, 0.5 M) was poured onto the GND-modified electrode, and the combination was incubated at 40 °C to concentrate the potassium ferricyanide solution.
(2) A glucose oxide (GOx) solution (20 μL, 2 U μL^{-1}) was dropped onto the biosensor, and the combination was incubated at 40 °C for 1 h.
(3) A Nafion thin film was produced by dropping 10 μL of a Nafion solution (2 wt%) onto the GOx immobilized electrode.

The SP-150 potentiostat (Bio-Logic, USA) used for the detection of the effective sensing areas was employed for the glucose concentration detection. A 0.1-M phosphate buffer saline (PBS) with pH 7.4 and 0.05-M $K_4Fe(CN)_6$ mixing electrolyte was used as the electrolyte.

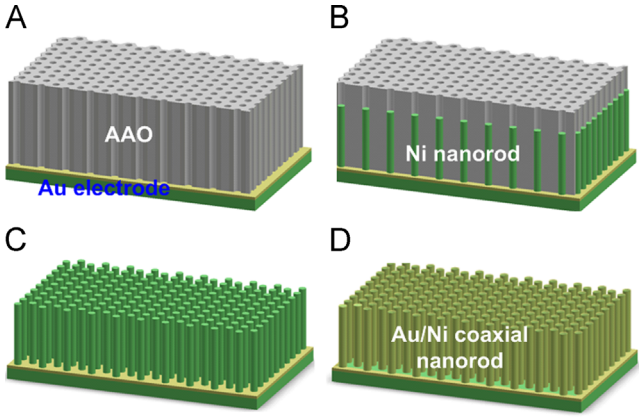

Fig. 2. Schematic representation of the fabrication procedure. (A) Working electrode coating; (B) nickel electroforming; (C) alumina etching; (D) immersion gold and annealing.

3. Results and discussions

3.1. Au–Ni coaxial nanorod array fabrication results

Fig. 3 illustrates the SEM images of the synthesized Ni nanorod arrays and the Au–Ni coaxial nanorod array. The diameter of the as-synthesized Ni nanorod was estimated to be 150 nm. After the IG process, the diameter of the resulting Au–Ni nanorod was approximately 250 nm. The thickness of the additive Au shell was approximately 50 nm. The height of the synthesized coaxial nanorod was approximately 30 μm, and the average diameter of the nanorods was around 250 nm (0.25 μm). Hence, the aspect ratio was 120.

Before taking the SEM image, the sample had to be dried. During the drying process, the water cohesion led to the aggregation of the Au–Ni coaxial nanorods as shown in Fig. 3. To further verify that potassium ferricyanide, GOx, and Nafion polymer could penetrate to the surface of each Au–Ni coaxial nanorod, SEM image for the sample that had been sequentially attached potassium ferricyanide, GOx, and Nafion was taken (Fig. S1). It can be observed from Fig. S1 that potassium ferricyanide, GOx, and Nafion polymer could diffuse into the interspace of the Au–Ni coaxial nanorod array and adhere to the surface of each Au–Ni coaxial nanorod.

It has been reported that the sensitivity of a biosensor electrode increases with an increase in the electrode surface roughness (Qiu et al., 2009; Seker et al., 2009). Our Au–Ni coaxial nanorod array electrode as shown in Fig. 3(B) not only provided a higher surface roughness when compared with a flat Au electrode but also an enhanced effective sensing surface due to the total nanorod surface. The surface roughness of our Au–Ni coaxial nanorod array electrode was estimated in terms of the voltammetric reduction reaction during a CV process (Douglass et al., 2008; Trasatti and Petrii, 1992).

Fig. 4(A) and (B) displays the cyclic voltammograms for the Au–Ni coaxial nanorod array electrode and its corresponding current verse time curve, respectively. The area below the horizontal axis (zero current) shown in Fig. 4(B) represents the total electric charge required for a complete reduction on the electrode. The reduction area below the horizontal axis was calculated to be −8803 μC. Since a total charge of 390 μC was required for 1 cm^2 of Au electrode to form AuO, the effective sensing area of the fabricated Au–Ni coaxial nanorod array electrode was estimated to be 22.57 cm^2 (8803/390). This was approximately 79.8 times that of the ϕ=6 mm hole.

The quality of an electrochemical biosensor can be represented in terms of the electron diffusion speed on its electrode surface. A fast electron diffusion speed implies that an efficient charge transfer through the interface between the solution and electrode surface can be achieved. The Randles–Sevcik equation shown below was adopted for electron diffusion speed estimation

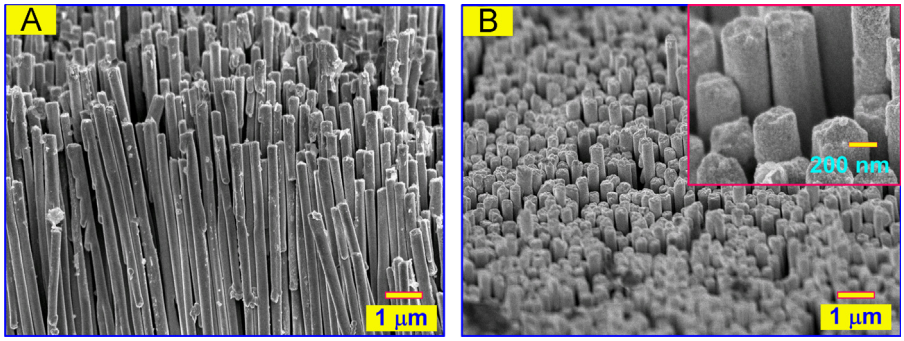

Fig. 3. SEM images of the nickel nanorod array (A) and the Au–Ni coaxial nanorod array (B) after 3 min of IG.

through CV.

$$i_p = 2.69 \times 10^5 \times n^{3/2} \times A \times C \times D^{1/2} \times v^{1/2} \quad (1)$$

where i_p denotes the current peak height of the voltammogram; n, the number of electrons appearing in a half-reaction for the redox couple; A, the area of the electrode (cm^2); C, the concentration of the analyte (mol cm^{-3}); D, the diffusivity of the analyte; and v, the potential scan rate (100 mV s^{-1}). Assuming n, A, C, and D are kept fixed, i_p is proportional to the square root of the scanning rate.

Fig. 4(C) displays the cyclic voltammograms for the Au–Ni coaxial nanorod array electrode for various scan rates from 30 to 400 mV s^{-1} using a 0.1-M PBS and 0.05-M $K_4Fe(CN)_6$ mixing electrolyte. The polarization overpotential (ΔE_p) that denotes the difference between the oxidation peak (E_{pa}) and the reduction peak (E_{pc}) for a certain scan rate increases with an increase in the scan rate. The linear relationships between the redox peak current and the square root of the scan rate of the proposed nanorod array electrode and the flat Au electrode are plotted in Fig. 4(D). It can be observed that the slope for the nanorod array electrode is approximately thrice that of the flat Au electrode. This fact implies that the nanorod array electrode enables rapid electron diffusion.

3.2. Glucose detection results

The performance of the proposed device with respect to glucose detection is illustrated in Fig. 5. Fig. 5(A) shows the cyclic voltammograms for various glucose concentrations using the electrode made of Au–Ni coaxial nanorod arrays. The average overpotential (ΔE_p) for five different glucose concentrations (0.0275–27.5 mM) was calculated to be 0.36 V. In addition, the mA peak currents implied that the charge transfer density in the proposed electrode was highly enhanced. Further, we rearranged the data displayed in Fig. 5(A) and plotted the relationship between i_{pa} and the glucose concentration as shown in the inset. Each measurement was conducted five times. The linear detection range was 27.5 μM to 27.75 mM with a high R^2 value of 0.9934. The sensitivity of the proposed glucose biosensor was calculated to be 778.2 μA mM^{-1} cm^{-2}, and the detection limit was 5.5 μM. The demonstrated extremely high sensitivity could be ascribed to the large effective sensing area of the Au–Ni nanorod array electrode, which could attach a considerable amount of GOx protein for more extensive glucose oxidation.

It has been reported that nickel nanorods could be modified and used as the electrode for a non-enzyme glucose biosensor (Guo et al., 2013). The nickel nanorod array was oxidized to NiO nanorod array at a high temperature condition (300 °C) and then used for glucose detection by CV in a NaOH solution. Although our Au–Ni coaxial nanorod array had not been subjected to a high temperature oxidation process and the electrolyte for glucose detection was not the NaOH solution, further experiments were conducted to examine whether the Ni core of the nickel nanorod affected the glucose detection results. Various glucose concentrations (2.75, 5.5 and 11.1 mM) were detected using the Au–Ni coaxial nanorod array electrode without GOx coating. The resulting cyclic voltammograms are illustrated in Fig. S2. It can be observed that the redox peak currents for these three concentrations are almost identical. The results indicate that our Au–Ni coaxial nanorods do not react with glucose and the detecting signal was from the reactions between the GOx and glucose.

Fig. 5(B) shows the amperometry results for various glucose concentrations in the case of the Au–Ni coaxial nanorod array electrode. The sensor chip was immersed into glucose of various concentrations. A constant DC potential of 0.4 V was applied, and the trajectories of current along with the processing time were recorded. The steady state at 13 s could be observed. Since the effective sensing area of our Au–Ni coaxial nanorod array was relatively large, the initial current was very high. A relatively long time was required to achieve the steady state. The relationship between the measured current density (μA cm^{-2}) and the glucose concentration (mM) was plotted and displayed in the inset

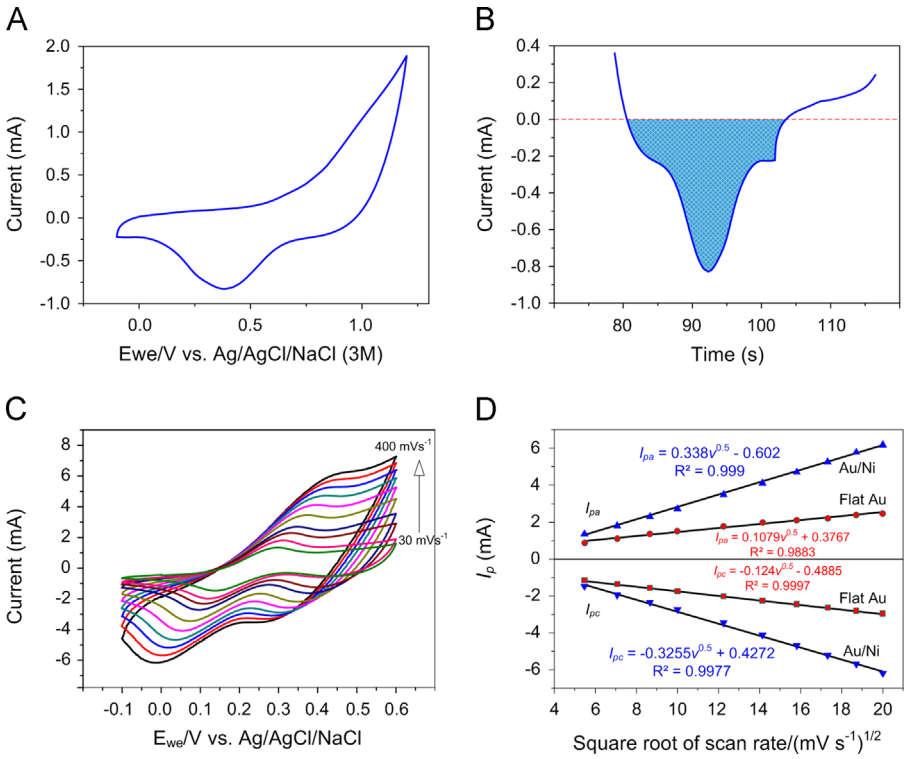

Fig. 4. Electrode characterizations by cyclic voltammetry in a 0.1-M PB solution (pH 7.0). (A) Cyclic voltammetry (i–v) with a scan rate of 50 mV s^{-1}; (B) cyclic voltammetry (i–t); (C) cyclic voltammetry of various scan rates for the Au–Ni coaxial nanorod arrays electrodes; (D) linear relationship between the redox peak current and the square root of the scan rate.

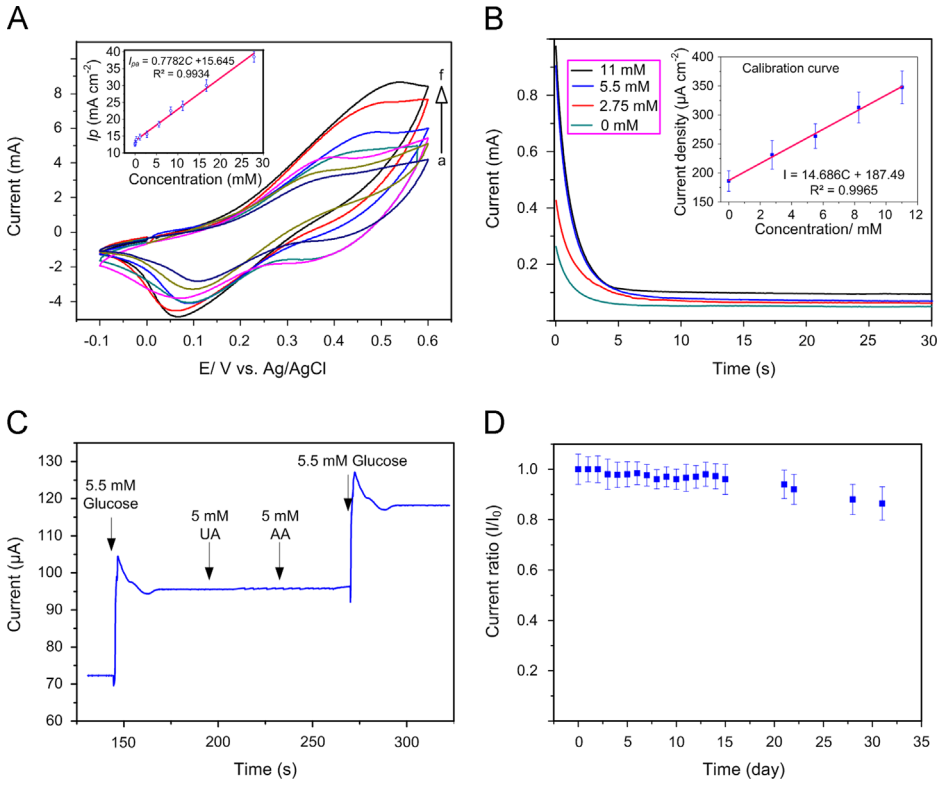

Fig. 5. Glucose detection results. (A) Cyclic voltammogram for various glucose concentrations with curves *a* to *f* representing the concentrations of 0, 0.0275, 5.5, 11, 16.65, and 27.5 mM, respectively. (inset) Linear calibration curve representing the peak current and concentration relationship; (B) amperometrics for different glucose concentrations with 0, 2.75, 5.5, and 11 mM. (inset) Linear calibration curve represents the relationship between the steady-state current and glucose concentration; (C) response of the Au–Ni coaxial nanorod array electrode to sequential injections of 5.5 mM glucose, 5 mM UA, 5 mM AA, and 5.5 mM glucose; (D) long-term stability test for 5.5-mM glucose over a period of 30 days.

Table 1
Nanostructure-based glucose biosensors and their functional properties.

Electrode	**Sensitivity** (μA mM^{-1} cm^{-2})	**Detection limit** (μM)	**Linear range** (mM)	**Reference no**
CS/GOx–PABA–Au_{nano}/Au-plated Au	97.7	0.1	0.002–3.7	Huang et al. (2012)
GOx–AuNPs/ESM		3.50	0.0083–0.966	Zheng et al. (2011)
Au–dithiol/Au–cystamine/GOx	8.8	8.2	0.020–5.7	Zhang et al. (2005)
Au nanodendrite	46.76	7	0.028–8.4	Liu et al. (2013a)
Nafion–graphene–Pd modified GC		1	0.01–5	Lu et al. (2011)
GOD–graphene–chitosan	37.93	20	0.08–12	Kang et al. (2009)
PtRu(1:1)–MWNT–IL/GCE	10.7	50	0.2–15	Xiao et al. (2009)
Nafion–silica/MWNT–g–PANI/GOx	5.01	0.1	1–10	Gopalan et al. (2009)
Nano NiO	55.9 and 66	0.16	0.001–0.110 1–10	Mu et al. (2011)
Cu_2O/GNs		20.8	0.3–7.8	Liu et al. (2013b)
GOD/MAA/AuNPs/TiO_2NT/Ti		310	0.4–8	Zhang et al. (2011)
Au–Ni coaxial nanorad array	**778.2**	**5.5**	**0.0275–27.75**	**This work**

of Fig. 5(B). Each measurement was repeated three times. A good linearity was illustrated by the R^2 value of 0.9965. Au–Ni coaxial nanorod array electrodes without Nafion were further implemented for the amperometry experiments. The results are shown in Fig. S3 with the relationship between the measured current density (at 13 s) and the glucose concentration being plotted and displayed in the inset of Fig. S3. When compared with Fig. 5(B), it can be found the redox peak current for the glucose of the same concentrations detected using an electrode without coating Nafion is larger than that of a Nation coated electrode. Interference of other substances such as uric acid (UA) and ascorbic acid (AA) in human's blood can degrade the efficacy of a glucose sensing device. In this study, Nafion was used to prevent the interference happening. To verify the selectivity, the response of the Au–Ni coaxial nanorod array electrode to sequential injections of 5.5 mM glucose, 5 mM uric acid (UA), 5 mM ascorbic acid (AA), and 5.5 mM glucose in an oxygen-containing PBS solution was examined. Fig. 5(C) illustrates the results of the selectivity test. The results indicate that the proposed sensing device is free from the interference of UA and AA. Besides the features such as sensitivity, detection limit, linear range, and selectivity, long-term stability is another pivotal requirement of a glucose biosensor. The glucose biosensors were stored dry at 4 °C for a successive stability test over a period of 30 days. Fig. 5(D) displays the long-term investigation results for the glucose concentration of 5.5 mM. The measured peak current dropped by approximately 13%. The degradation of the GOx activity was a possible cause of this degeneration.

In recent years, nanostructured electrodes have been widely used in diabetes detection devices because of their significant characteristics such as high surface area, high surface activity, high catalytic efficiency, and strong adsorption. A comparison of the functional properties of the Au–Ni coaxial nanorod array electrode

in this study with those of the recently developed nanostructure glucose biosensors in terms of sensitivity, detection limit, and linear range is summarized in Table 1. Overall, the Au–Ni coaxial nanorod array electrode used in this study exhibited good functional properties.

4. Conclusion

Because of its high biocompatibility, gold, particularly the various nanostructures of gold, has been widely used in biomedical applications. A high-aspect-ratio gold nanorod that has a large surface-to-volume ratio is more suitable for biomedical applications. Considering both mechanical properties and bio-compatibility, we proposed a novel approach for the fabrication of a highly sensitive Au–Ni coaxial nanorod array electrode by integrating nano electroforming and the immersion gold (IG) method.

The average diameter of the synthesized Ni nanorods was estimated to be 150 nm. After the IG process, the average diameter of the resulting Au–Ni nanorods was approximately 250 nm. The thickness of the additive Au shell was approximately 50 nm. Since the height of the synthesized coaxial nanorod was approximately 30 μm, the aspect ratio was 120. Compared to the already reported Au nanorod arrays having an aspect ratio of only around 20, our Au–Ni nanorod array could provide an enhanced effective sensing area. Actual glucose measurements revealed that the proposed biosensing scheme could operate in a linear range of 27.5 μM–27.5 mM with a high sensitivity of 778.2 μA mM^{-1} cm^{-2}. Long-term stability of the proposed device was confirmed through 30-day investigation.

Acknowledgement

The authors would like to offer their thanks to the National Science Council of Taiwan under grant number NSC-101-2212-E-005-022-MY3 for their financial support of this research.

Appendix A. Supporting information

Supplementary data associated with this article can be found in the online version at http://dx.doi.org/10.1016/j.bios.2014.01.023.

References

Clark, L.C., Lyons, C., 1962. Ann. N.Y. Acad. Sci. 102 (1), 29–45.
Crouch, E., Cowell, D.C., Hoskins, S., Pittson, R.W., Hart, J.P., 2005. Biosens. Bioelectron. 21 (5), 712–718.
Danaei, G., Finucane, M.M., Lu, Y., Singh, G.M., Cowan, M.J., Paciorek, C.J., Lin, J.K., Farzadfar, F., Khang, Y.-H., Stevens, G.A., 2011. Lancet 378 (9785), 31–40.
Douglass , E.F., Driscoll, P.F., Liu, D., Burnham, N.A., Lambert, C.R., McGimpsey, W.G., 2008. Anal. Chem. 80 (20), 7670–7677.
Gopalan, A.I., Lee, K.P., Ragupathy, D., Lee, S.H., Lee, J.W., 2009. Biomaterials 30 (30), 5999–6005.
Guo, C.-Y., Wang, Y.-M., Zhao, Y.-Q., Xu, C-l, 2013. Anal. Methods
Hill, H.A., Higgins, I.J., McCann, J.M., Davis, G., 1996. Strip Electrode Including Screen Printing of a Single Layer. Google Patents.
Huang, Y., Qin, X., Li, Z., Fu, Y., Qin, C., Wu, F., Su, Z., Ma, M., Xie, Q., Yao, S., 2012. Biosens. Bioelectron. 31 (1), 357–362.
Kang, X., Wang, J., Wu, H., Aksay, I.A., Liu, J., Lin, Y., 2009. Biosens. Bioelectron. 25 (4), 901–905.
Lee, S., Ringstrand, B.S., Stone, D.A., Firestone, M.A., 2012. ACS Appl. Mater. Interfaces 4 (5), 2311–2317.
Liu, H.-C., Tsai, C.-C., Wang, G.-J., 2013a. Nanotechnology 24 (21), 215101.
Liu, M., Liu, R., Chen, W., 2013b. Biosens. Bioelectron.
Lu, L.-M., Li, H.-B., Qu, F., Zhang, X.-B., Shen, G.-L., Yu, R.-Q., 2011. Biosens. Bioelectron. 26 (8), 3500–3504.
Luo, J., Luo, P., Xie, M., Du, K., Zhao, B., Pan, F., Fan, P., Zeng, F., Zhang, D., Zheng, Z., 2013. Biosens. Bioelectron.
Marx, S., Jose, M.V., Andersen, J.D., Russell, A.J., 2011. Biosens. Bioelectron. 26 (6), 2981–2986.
Mu, Y., Jia, D., He, Y., Miao, Y., Wu, H.-L., 2011. Biosens. Bioelectron. 26 (6), 2948–2952.
Nagata, R., Yokoyama, K., Clark, S.A., Karube, I., 1995. Biosens. Bioelectron. 10 (3), 261–267.
Qiu, C., Wang, X., Liu, X., Hou, S., Ma, H., 2012. Electrochim. Acta 67, 140–146.
Qiu, H., Xue, L., Ji, G., Zhou, G., Huang, X., Qu, Y., Gao, P., 2009. Biosens. Bioelectron. 24 (10), 3014–3018.
Seker, E., Reed, M.L., Begley, M.R., 2009. Materials 2 (4), 2188–2215.
Trasatti, S., Petrii, O., 1992. J. Electroanal. Chem. 327 (1), 353–376.
Turner, A.P., Chen, B., Piletsky, S.A., 1999. Clin. Chem. 45 (9), 1596–1601.
Wang, J., 2008. Chem. Rev. 108 (2), 814–825.
Whitney, T., Searson, P., Jiang, J., Chien, C., 1993. Science 261 (5126), 1316–1319.
Xiao, F., Zhao, F., Mei, D., Mo, Z., Zeng, B., 2009. Biosens. Bioelectron. 24 (12), 3481–3486.
Zhang, S., Wang, N., Yu, H., Niu, Y., Sun, C., 2005. Bioelectrochem. 67 (1), 15–22.
Zhang, Z., Xie, Y., Liu, Z., Rong, F., Wang, Y., Fu, D., 2011. J. Electroanal. Chem. 650 (2), 241–247.
Zheng, B., Xie, S., Qian, L., Yuan, H., Xiao, D., Choi, M.M., 2011. Sens. Actuators, B 152 (1), 49–55.